W. Stuiver *
R. S. McDuffie

Analysis and Numerical Calculations of the Dynamic Behavior of Plane Pivoted Slider Bearings†

Abstract: The dynamic behavior of plane, self-acting, pivoted slider bearings of infinite length is examined for the case of an incompressible lubricating film. The equations of motion for the slider are derived, with the lubricant force expressed in terms of the motion-coordinates and their derivatives and of the parameters that characterize the system. Equilibrium positions of the system are determined numerically and the stability of small motions in the neighborhood of these positions is examined. The nature of large motions is investigated by numerical integration of the equations of motion, and the transient behavior of the system is shown and discussed for some specific cases.

Introduction

In the past few decades numerous investigators have studied the problems of stability and motion of bearing systems supported by a fluid film. Most of the published work in this field relates to the behavior of cylindrical journal bearings,[1,2] presumably because of their importance in practical applications; in comparison, the dynamic behavior of pivoted slider bearings has received scant attention except for extensive studies of the dynamic properties of the fluid film for a prescribed clearance between the bearing surfaces.[3,4,5] The purpose of the present paper is to describe an attempt to begin to fill this gap and to contribute to further work, both analytical and numerical, on the problems of motion of slider bearings.

Although the bearing system considered in this paper is a considerably simplified model of actual configurations, the results of the work are believed to be of more than academic interest. The main simplifications it involves derive from the assumptions of infinite length of the slider and incompressibility of the lubricant. For an arbitrary kinematic condition of the slider, these assumptions allow us to perform analytical integration of the Reynolds equation for the pressure distribution in the lubricant and to calculate the corresponding force and moment exerted upon the slider. The mathematical formulation of the problem of motion is thereby reduced to a set of two simultaneous ordinary differential equations of second order in the motion coordinates of the slider. These equations contain the reactions of both the lubricant and the bearing suspension system, the former being represented by highly nonlinear damping and restoring functions of the motion coordinates and their derivatives. The equations are used for the determination of equilibrium positions of the slider for various values of the system parameters, for the investigation of the stability of small motions near these positions, and for the numerical calculation of some specific motion trajectories.

It is believed that the results of this study will contribute to a further understanding of the dynamic bebehavior of actual sliders, and in particular to knowledge of their response to disturbances from equilibrium and the effects of modifications in system configuration. The results can also serve as a check and, perhaps, a point of departure for computer programs for the solution of the much more complex problem of motion of slider bearings with a compressible lubricant.

* Department of Mechanical Engineering, University of Hawaii, Honolulu, Hawaii.
† This work was supported in part by the Office of Naval Research under Contract Nonr 3448(00), Task Nr 061-120.

Notation

Symbol	*Referent*
B	Breadth of slider
F	Lubricant friction force per unit length on slider
I	Moment of inertia of slider per unit length around center of mass
K	Spring force per unit length on slider
M	Lubricant pressure moment per unit length on slider around pivot point
Q	Rotational spring moment per unit length on slider around pivot point
U	Speed of driving surface
W	Lubricant pressure force per unit length on slider
b	Distance along slider from pivot point to trailing edge
d_1	Distance along slider from pivot point to center of mass
x	Distance in direction of driving surface motion
$h(x)$	Clearance between slider and driving surface
h_1	Clearance at pivot point
m	Mass per unit length of slider
p	Lubricant pressure
p_a	Ambient pressure
ϕ	p/p_a
t	Time
ω	$\sqrt{p_a/m}$
τ	ωt
β	h_1/b
β_0	β at equilibrium
h_0	$\beta_0 b$
ξ	x/b
ϵ	Angle of slider with respect to driving surface
ϵ_0	ϵ at equilibrium
X	ϵ/β
X_0	ϵ_0/β_0
ζ	$\beta - \beta_0$
η	$\epsilon - \epsilon_0$
θ	$h(x)/b$
γ	$K'(h_0)/p_a$
ψ	$Q'(\epsilon_0)/B^2 p_a$
μ	Viscosity of lubricant
α	b/B
δ	d_1/b
κ	$(6\mu U)/Bp_a\ (= \alpha^2\beta_0^2\Lambda)$
λ	$(12\mu\omega)/p_a\ (= \alpha^2\beta_0^2\Sigma)$
σ	$(I + md_1^2)/mb^2 = (1/12\alpha^2) + \delta^2$
Π	$[K(b_0) - b_0K'(h_0)]/Bp_a$
Φ	$-[Q(\epsilon_0) - \epsilon_0 Q'(\epsilon_0)]/B^2 p_a$

Part 1: Analysis of the dynamical problem

• *Equations of motion for the slider*

We are here concerned with the model of an infinitely long plane slider which is loaded by a linear spring as shown in Fig. 1. The spring is connected to the slider surface at a pivot point whose movement is constrained to a vertical path. Motion of the slider around the pivot point is restrained by a rotary spring that is also assumed to be linear. The assumption of linearity of both system springs is technically justified since their force-displacement curves are smooth enough to be replaced by linear approximations over the relatively minute range of bearing motion that is involved. On the other hand, since the speeds of the bearing motion components are not necessarily small and the damping in the mechanical suspension system cannot be correspondingly simplified, we neglect the influences of damping in the suspension system to maintain a rigorous model and achieve simplicity.

The driving surface of the bearing is assumed to move horizontally with constant speed U, and to have no vertical velocity component. While not essential, this assumption of constant velocity of the driving surface will permit mathematical convenience. By restricting the analysis to plane bearing surfaces we are able to express the dynamical problem simply in terms of the motion coordinates and the parameters that characterize the system.

In the model the action of the lubricant upon the slider can be represented by W, the resultant of the pressure acting normal to the face of the slider, and F, the resultant of the shearing stresses acting along the slider surface. It is not necessary to consider the latter force because it can be shown[4] to be of order of ϵ, where ϵ is the inclination angle of the slider; hence, the vertical component of F is

Figure 1 **Geometry of the bearing configuration.**

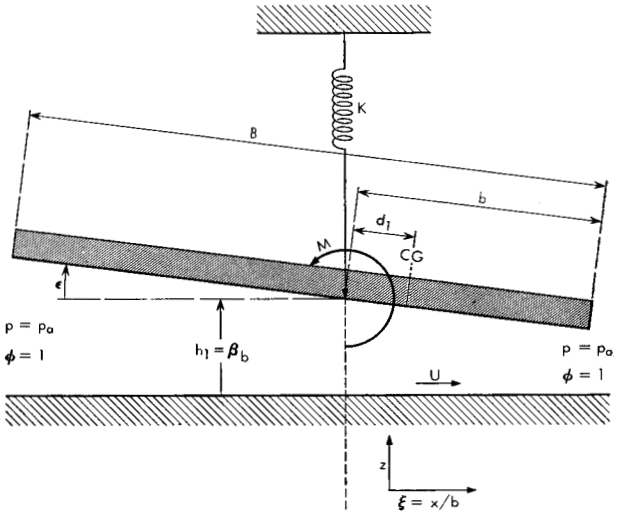

a quantity of the order of ϵ^2. Furthermore, we assume that the center of gravity (CG) is located along the face of the slider so that there is no moment-component around this point due to F.

As seen in Fig. 1, the coordinate z of CG is given by

$$z = h_1 - d_1 \sin \epsilon, \tag{1}$$

where h_1 is the coordinate of the pivot. Neglecting terms of order ϵ and smaller and letting K be the spring force, M be the moment about the pivot point due to the film pressure, and Q be the loading moment about the pivot point, we derive the two equations of motion

$$m[\ddot{h}_1 + d_1(\epsilon\dot{\epsilon}^2 - \ddot{\epsilon})] = W - K, \tag{2}$$

expressing force-equilibrium along the translation direction of the pivot point, and

$$I\ddot{\epsilon} = -M - Q + (W - K)d_1, \tag{3}$$

expressing moment-equilibrium around the center of gravity. (In both expressions, dots indicate differentiation with respect to t.) Henceforth, we assume linearity of the springs, i.e.,

$$\begin{aligned} K &= K(h_0) + K'(h_0)\cdot(h_1 - h_0) \\ &= [K(h_0) - h_0 K'(h_0)] + K'(h_0)h_1, \end{aligned} \tag{4}$$

where h_0 is the coordinate of the pivot at equilibrium, and

$$\begin{aligned} Q &= Q(\epsilon_0) + Q'(\epsilon_0)(\epsilon - \epsilon_0) \\ &= [Q(\epsilon_0) - \epsilon_0 Q'(\epsilon_0)] + Q'(\epsilon_0)\epsilon, \end{aligned} \tag{5}$$

where ϵ_0 is the equilibrium angle, and primes indicate differentiation with respect to the argument. In addition we assume that the term $\epsilon\dot{\epsilon}^2$ in (2) may be neglected in comparison with $\ddot{\epsilon}$.

For purposes of convenience, we transform the equations of motion (2) and (3) into dimensionless form. We define $\omega = \sqrt{p_a/m}$ and $\tau = \omega t$. The motion coordinate h_1 and d_1 are normalized with respect to b by $h_1 = \beta b$ and $d_1 = \delta b$. The equations of motion then become

$$\ddot{\beta} - \delta\ddot{\epsilon} = \frac{W}{\alpha B p_a} - \left(\frac{\Pi}{\alpha} + \gamma\beta\right), \tag{6}$$

$$(\sigma - \delta^2)\ddot{\epsilon} = \frac{-M}{\alpha^2 B^2 p_a} + \frac{W\delta}{\alpha B p_a} + \frac{\Phi - \psi\epsilon}{\alpha^2} - \delta\left(\frac{\Pi}{\alpha} + \gamma\beta\right). \tag{7}$$

In Eqs. (6), and (7) and hereafter, dots indicate differentiation with respect to τ. Multiplying Eq. (6) by δ and subtracting (7) yields

$$\delta\ddot{\beta} - \sigma\ddot{\epsilon} = \frac{M}{\alpha^2 B^2 p_a} - \frac{\Phi - \psi\epsilon}{\alpha^2}. \tag{8}$$

Henceforth we shall deal with Eqs. (6) and (8).

• *Lubricant action upon the slider*

The effect of the lubricant on the motion of the slider is represented by the factors $W/\alpha\, Bp_a$ and $M/\alpha^2 B^2 p_a$ in (6) and (8). These factors represent the resultant film force and moment around the pivot point due to the pressure distribution in the lubricant. This pressure distribution is governed by the well-known Reynolds equation

$$(h^3 p_x)_x = 6\mu\, U h_x + 12\mu h_t. \tag{9}$$

Note that (9) is obtained from the equations of conservation of mass and momentum of the lubricant, using an order-of-magnitude analysis of the individual terms in the expression for momentum to show that the fluid inertia forces are negligible. Detailed derivations of (9) can be found in Reference 5 and elsewhere in the literature.

With the substitutions

$$h = \theta b, \qquad p = \phi p_a, \qquad x = \xi b, \tag{10}$$

we can write (9) in dimensionless form

$$\alpha(\theta^3\phi_\xi)_\xi = \kappa\theta_\xi + \lambda\theta_\tau\alpha, \tag{11}$$

where parameters κ and λ are defined as

$$\kappa = \frac{6\mu\, U}{Bp_a}, \qquad \lambda = \frac{12\mu\omega}{p_a}. \tag{12}$$

These parameters are related to the bearing and squeeze numbers Λ and Σ, often used in gas lubrication analyses, by the equations

$$\Lambda = \kappa\left(\frac{B}{h_0}\right)^2, \qquad \Sigma = \lambda\left(\frac{B}{h_0}\right)^2, \tag{13}$$

where $h_0 = \beta_0 b$. The film thickness is given by

$$h = h_1 - x \tan \epsilon. \tag{14}$$

By using the substitutions of (10) and

$$h_1 = \beta b, \ \epsilon = \beta X \tag{15}$$

and recalling that higher order terms in ϵ are neglected in our approach, we obtain the normalized expression for film thickness

$$\theta = \beta - \xi\epsilon = \beta(1 - \xi X). \tag{16}$$

Now (11) can be written as

$$\alpha[\beta^3(1 - \xi X)^3\phi_\xi]_\xi = -\kappa\epsilon + \lambda(\dot{\beta} - \xi\dot{\epsilon})\alpha \tag{17}$$

and we find directly by integration over ξ,

$$\phi_\xi = -\frac{C_0 + (\kappa\epsilon - \alpha\lambda\dot{\beta})\xi + \alpha\lambda\dot{\epsilon}(\xi^2/2)}{\alpha\beta^3(1 - \xi X)^3}, \tag{18}$$

where C_0 represents a constant of integration. We shall use (18) for deriving the normalized pressure ϕ as a func-

tion of the independent variable ξ, the motion coordinates β, ϵ and their derivatives $\dot{\beta}$, $\dot{\epsilon}$, and the parameters that characterize our model. The expressions for the film force W, and moment M around the pivot point then follow immediately by integration over ξ.

The pressure, ϕ, may be expressed as a function of ξ

$$\phi = \phi_0 - \frac{1}{\alpha\beta^3}\int_{\xi_0}^{\xi} \frac{C_0 + (\kappa\epsilon - \alpha\lambda\dot{\beta})\xi + (\alpha\lambda\dot{\epsilon}\xi^2)/2}{(1 - \xi X)^3}\, d\xi, \tag{19}$$

where $\xi_0 = -(1 - \alpha)/\alpha$; hence we have the expression

$$\phi(\xi) = \phi_0 - \frac{1}{2\alpha\epsilon^3}\Big[\{C_0 X^2 - (\kappa\epsilon - \alpha\lambda\dot{\beta})X - \tfrac{3}{2}\alpha\lambda\dot{\epsilon} + 2[(K\epsilon - \alpha\lambda\dot{\beta})X + \alpha\lambda\dot{\epsilon}]\xi X\}/(1 - \xi X)^2 - \alpha\lambda\dot{\epsilon}\ln(1 - \xi X)\Big], \tag{20}$$

with $X = \epsilon/\beta$.

The integration constants C_0 and ϕ_0 are obtained from the condition that the pressure must be ambient at the bearing ends. In view of our definitions, these boundary conditions assume the form

$$\phi\left(-\frac{1 - \alpha}{\alpha}\right) = 1 = \phi(1). \tag{21}$$

The calculation of the constants C_0 and ϕ_0 from (20) and (21) is a laborious procedure which need not be given. It is necessary only to mention that substitution in (20) of the resulting expressions for these constants, which are functions of the motion coordinates and their derivatives, yields for ϕ an expression of the form

$$\phi = 1 + \Phi(\xi;\ \beta,\ \epsilon,\ \dot{\beta},\ \dot{\epsilon};\ \alpha,\ \kappa,\ \lambda), \tag{22}$$

where Φ is a complicated function which is strongly dependent on the factor X, that is, on the ratio ϵ/β. It may be easily verified from the geometry of the model of Fig. 1 that all possible motions of the slider are those in the region

$$-\frac{\alpha}{1 - \alpha} \leq X \leq 1, \tag{23}$$

where the end-values represent contact between the slider and the driving surface at the bearing ends. It follows from (22) that the pressure distribution along the face of the slider is given by

$$p = p_a\left[1 + \Phi\left(\frac{x}{\alpha B};\ \beta,\ \epsilon,\ \dot{\beta},\ \dot{\epsilon};\ \alpha,\ \kappa,\ \lambda\right)\right], \tag{24}$$

and is a function, of course, of the kinematic condition of the slider.

The force and moment exerted upon the slider by the lubricant follow directly from (24). Since the pressure above the slider is ambient, we have

$$W = \int_{-B+b}^{b} (p - p_a)\, dx = \alpha B p_a \int_{-(1-\alpha)/\alpha}^{1} (\phi - 1)\, d\xi \tag{25}$$

and

$$M = \int_{-B+b}^{b} (p - p_a)x\, dx = \alpha^2 B^2 p_a \int_{-(1-\alpha)/\alpha}^{1} (\phi - 1)\xi\, d\xi. \tag{26}$$

Substitution of the expression (24) in (25) and (26) yields the force, W, and the moment, M, around the pivot point as functions of the motion coordinates, β and ϵ, and their derivatives, $\dot{\beta}$ and $\dot{\epsilon}$, and the parameters α, κ and λ. We omit the details of this calculation and present only the final expressions for force and moment, respectively,

$$W = \alpha B p_a\left[\frac{\kappa\epsilon - \alpha\lambda\dot{\beta}}{\beta\epsilon^2}\cdot c(\alpha,\ X) + \frac{\lambda\dot{\epsilon}}{\beta^2\epsilon}\cdot d(\alpha,\ X)\right] \tag{27}$$

and

$$M = \alpha^2 B^2 p_a\left[\frac{\kappa\epsilon - \alpha\lambda\dot{\beta}}{\epsilon^3}\cdot e(\alpha,\ X) + \frac{\lambda\dot{\epsilon}}{\beta\epsilon^2}\cdot f(\alpha,\ X)\right]. \tag{28}$$

The symbol X represents the ratio ϵ/β, and the functions $c(\alpha, X)$, $d(\alpha, X)$, $e(\alpha, X)$ and $f(\alpha, X)$ are given in Appendix 1. The expressions for the functions $c(\alpha, X)$ and $e(\alpha, X)$ were verified by comparison with expressions obtained independently for pressure force and moment for the stationary slider.[4] For the functions $d(\alpha, X)$ and $f(\alpha, X)$ such verification was not possible.

• *Positions of equilibrium and the stability of small motions*

This study of the dynamic behavior of the slider is based on the differential equations of motion obtained from (6) and (8) using force and moment equations of (27) and (28). The equations of motion assume the form

$$\ddot{\beta} - \delta\ddot{\epsilon} + \alpha\lambda\cdot\frac{c(\alpha,\ X)}{X^2}\cdot\frac{\dot{\beta}}{\beta^3} - \lambda\cdot\frac{d(\alpha,\ X)}{X}\cdot\frac{\dot{\epsilon}}{\beta^3} - \kappa\cdot\frac{c(\alpha,\ X)}{X}\cdot\frac{1}{\beta^2} + \frac{\Pi}{\alpha} + \gamma\beta = 0 \tag{29}$$

and

$$\delta\ddot{\beta} - \sigma\ddot{\epsilon} + \alpha\lambda\cdot\frac{e(\alpha,\ X)}{X^3}\cdot\frac{\dot{\beta}}{\beta^3} - \lambda\cdot\frac{f(\alpha,\ X)}{X^2}\cdot\frac{\dot{\epsilon}}{\beta^3} - \kappa\cdot\frac{e(\alpha,\ X)}{X^2}\cdot\frac{1}{\beta^2} + \frac{\Phi - \psi\epsilon}{\alpha^2} = 0. \tag{30}$$

The terms $[\kappa/\beta^2]\cdot[c(\alpha, X)/X]$ and $[\kappa/\beta^2]\cdot[e(\alpha, X)/X^2]$ may be interpreted as the "spring" reaction of the lubricant against, respectively, the vertical translation and rotation of the slider. Furthermore, the terms $[\lambda/\beta^3]\cdot[\alpha\cdot c(\alpha, X)/X^2]\cdot\dot{\beta}$ and $[\lambda/\beta^3]\cdot[d(\alpha, X)/X]\cdot\dot{\epsilon}$ in (29), and $[\lambda/\beta^3]\cdot[\alpha e(\alpha, X)/X^3]\cdot\dot{\beta}$ and $[\lambda/\beta^3]\cdot[f(\alpha, X)/X^2]\cdot\dot{\epsilon}$ in (30) may be interpreted as the "damping" reaction of the lubricant that is due to translation and rotational motion of the slider against its vertical motion and rotation around the pivot point, respectively.

The functions $d(\alpha, X)/X$ and $f(\alpha, X)/X^2$, not hitherto given in the literature, can be checked for small values of X. From (18) we find directly for $X = O(\epsilon)$,

$$\phi_\xi = -\frac{1}{\alpha\beta^3}\left[C_0 + (\kappa\epsilon - \alpha\lambda\dot{\beta})\xi + \frac{\alpha\lambda\dot{\epsilon}}{2}\cdot\xi^2\right]. \tag{31}$$

Hence

$$\phi = \phi_0 - \frac{1}{\alpha\beta^3}\left[C_0\xi + (\kappa\epsilon - \alpha\lambda\dot{\beta})\cdot\frac{\xi^2}{2} + \alpha\lambda\dot{\epsilon}\cdot\frac{\xi^3}{6}\right]. \tag{32}$$

The integration constants C_0 and ϕ_0 are again obtained from the boundary conditions (21). The corresponding lubricant force, W, and lubricant moment, M, exerted upon the slider for smaller values of X follow directly from resulting expressions $\phi(\xi)$ by the integrations (25) and (26). Giving only the results of these calculations, we have

$$W = \alpha B p_a\left[\frac{\kappa\epsilon - \alpha\lambda\dot{\beta}}{12\alpha^4\beta^3} - \frac{(1 - 2\alpha)\lambda\dot{\epsilon}}{24\alpha^4\beta^3}\right] \tag{33}$$

and

$$M = \alpha^2 B^2 p_a\left\{-\frac{(1 - 2\alpha)(\kappa\epsilon - \alpha\lambda\dot{\beta})}{24\alpha^5\beta^3} + \frac{[1 + 15(1 - 2\alpha)^2]\lambda\dot{\epsilon}}{720\alpha^5\beta^3}\right\}. \tag{34}$$

To make these expressions agree with (27) and (28) we must have, of course, the relations

$$\lim_{X\to 0}\left[\frac{c(\alpha, X)}{X^2}\right] = \frac{1}{12\alpha^4}, \lim_{X\to 0}\left[\frac{e(\alpha, X)}{X^3}\right] = -\frac{1 - 2\alpha}{24\alpha^5} \tag{35}$$

and

$$\lim_{X\to 0}\left[\frac{d(\alpha, X)}{X}\right] = -\frac{1 - 2\alpha}{24\alpha^4},$$

$$\lim_{X\to 0}\left[\frac{f(\alpha, X)}{X^2}\right] = \frac{1 + 15(1 - 2\alpha)^2}{720\alpha^5}. \tag{36}$$

These limits agree well with numerical evaluations of the functions $c(\alpha, X)/X^2$, $e(\alpha, X)/X^3$, $d(\alpha, X)/X$, and $f(\alpha, X)/X^2$ near zero.

Since (29) and (30) are too involved for analysis of the dynamical problem, we first apply the simplifications of the theory of small motions and examine the stability of these motions near the equilibrium positions of the slider; thereafter, we shall investigate the nature of large motions by means of numerical techniques. The numerical integration procedure is discussed further in Part 2 and some typical results are presented there.

Let us denote the state of motion of the slider by the vector $(\beta, \epsilon, \dot{\beta}, \dot{\epsilon})$ in phase-space S. The rest positions in this space are given by the vectors $(\beta_0, \epsilon_0, 0, 0)$, the equilibrium-coordinates β_0 and ϵ_0 being functions of the parameters that characterize the system. These functions follow directly from (29) and (30) as the solutions $\beta_0(\kappa, \alpha, \Pi, \gamma, \Phi, \psi)$ and $\epsilon_0(\kappa, \alpha, \Pi, \gamma, \Phi, \psi)$ of the algebraic equations

$$\kappa\alpha\cdot\frac{c(\alpha, X_0)}{\epsilon_0\beta_0} = \Pi + \alpha\gamma\beta_0 \tag{37}$$

and

$$\kappa\alpha^2\cdot\frac{e(\alpha, X_0)}{\epsilon_0^2} = \Phi - \psi\epsilon_0. \tag{38}$$

In many applications the incremental external spring force $\gamma\beta_0$ and moment $\psi\epsilon_0$ are small compared with the "bias" force Π and moment Φ. It is reasonable, then, to consider the special case $\gamma = \psi = 0$. We combine (37) and (38) obtaining

$$\frac{\Phi\cdot c(\alpha, X_0)}{\Pi X_0} = \frac{\alpha\cdot e(\alpha, X_0)}{X_0^2} \tag{39}$$

for the equilibrium value X_0 as a function of the parameters α, Π and Φ. Either (37) or (38) may then be used for the determination of β_0 and ϵ_0. From (37) we find

$$\beta_0^2 = \alpha\cdot\frac{\kappa}{\Pi}\cdot\frac{c(\alpha, X_0)}{X_0}. \tag{40}$$

In this case, therefore, the dependence of the equilibrium-coordinates β_0 and ϵ_0 upon the physical properties of the system is a function of the parameter ratios κ/Π and Φ/Π. Again, it should be noticed that these results are valid only for the special case $\gamma = \psi = 0$; more general results can be obtained in a similar way directly from (37) and (38).

The criteria for the stability of small motions in the neighborhood of the equilibrium positions are obtained by linearizing the equations of motion with respect to the perturbation variables $\zeta = \beta - \beta_0$ and $\eta = \epsilon - \epsilon_0$. Linearized forms of (29) and (30) are thus obtained by means of the substitutions $\beta = \beta_0 + \zeta$, $\epsilon = \epsilon_0 + \eta$ and omission of all terms of order two and higher in ζ, η and their derivatives; furthermore, the relations (37) and (38)

are utilized. The final forms of the linearized equations of motion are given below. (In (41) and (42) and hereafter, *primes* are used to indicate differentiation with respect to X_0.)

$$\ddot{\zeta} - \delta\ddot{\eta} + \alpha\lambda\cdot\frac{c(\alpha, X_0)}{X_0^2}\cdot\frac{\dot{\zeta}}{\beta_0^3} - \lambda\cdot\frac{d(\alpha, X_0)}{X_0}\cdot\frac{\dot{\eta}}{\beta_0^3} + \kappa\left\{\left[2\cdot\frac{c(\alpha, X_0)}{X_0} + X_0\left(\frac{c(\alpha, X_0)}{X_0}\right)'\right]\frac{\zeta}{\beta_0^3} - \left(\frac{c(\alpha, X_0)}{X_0}\right)'\cdot\frac{\eta}{\beta_0^3}\right\} + \gamma\zeta = 0 \tag{41}$$

and

$$\delta\ddot{\zeta} - \sigma\ddot{\eta} + \alpha\lambda\cdot\frac{e(\alpha, X_0)}{X_0^3}\cdot\frac{\dot{\zeta}}{\beta_0^3} - \lambda\cdot\frac{f(\alpha, X_0)}{X_0^2}\cdot\frac{\dot{\eta}}{\beta_0^3} + \kappa\left\{\left[2\cdot\frac{e(\alpha, X_0)}{X_0^2} + X_0\left(\frac{e(\alpha, X_0)}{X_0^2}\right)'\right]\frac{\zeta}{\beta_0^3} - \left(\frac{e(\alpha, X_0)}{X_0^2}\right)'\cdot\frac{\eta}{\beta_0^3}\right\} - \frac{\psi\eta}{\alpha^2} = 0 \tag{42}$$

Equations (41) and (42) describe the motion of the slider near its positions of equilibrium (β_0, ϵ_0, 0, 0). The criteria for the stability of such motions follow directly from well-known theorems of the theory of linear differential equations.

Let us write Eqs. (41) and (42) as

$$\ddot{\zeta} - \delta\ddot{\eta} + \lambda(A\dot{\zeta} - B\dot{\eta}) + \kappa(C\zeta - D\eta) + \gamma\zeta = 0 \tag{43}$$

and

$$\delta\ddot{\zeta} - \sigma\ddot{\eta} + \lambda(P\dot{\zeta} - Q\dot{\eta}) + \kappa(R\zeta - S\eta) - \frac{\psi\eta}{\alpha^2} = 0. \tag{44}$$

Here, the coefficients A, B, C, D and P, Q, R, S are functions of the coordinates β_0, ϵ_0 (through $X_0 = \epsilon_0/\beta_0$) and the parameter α; the expressions for these functions are given in Appendix 2. After substitution of the trial solution $\zeta = \zeta_0 e^{\nu\tau}$, $\eta = \eta_0 e^{\nu\tau}$ we derive the characteristic equation

$$\nu^4 + a_1\nu^3 + a_2\nu^2 + a_3\nu + a_4 = 0 \tag{45}$$

with

$$a_1 = 12\alpha^2\lambda[Q + A\sigma - (B + P)\delta] \tag{46a}$$

$$a_2 = 12\alpha^2\left\{\kappa[S + C\sigma - (D + R)\delta] + \lambda^2(AQ - BP) + \frac{\alpha^2\gamma\sigma + \psi}{\alpha^2}\right\} \tag{46b}$$

$$a_3 = 12\alpha^2\left\{\kappa\lambda[(AS + CQ) - (BR + DP)] + \lambda\frac{\alpha^2\gamma Q + \psi A}{\alpha^2}\right\} \tag{46c}$$

$$a_4 = 12\alpha^2\left[\kappa^2(CS - DR) + \kappa\frac{\alpha^3\gamma S + \alpha\psi C + \gamma\psi}{\alpha^3}\right], \tag{46d}$$

using the definition $\sigma = (1/12\alpha^2) + \delta^2$. The imaginary parts of the roots ν of this equation represent the oscillatory character of small motions near the positions of equilibrium, and the real parts indicate growth or decay. The conditions for stability of these motions[6] are

$$a_1 > 0, \quad g = a_1a_2 - a_3 > 0, \quad a_3g - a_1^2a_4 > 0, \quad a_4 > 0 \tag{47}$$

or

$$a_1 > 0, \quad a_1a_2a_3 - a_3^2 - a_1^2a_4 > 0, \quad a_3 > 0, \quad a_4 > 0. \tag{48}$$

With the four expressions of (46) and those given in Appendix 2, the conditions of (47) and (48) can be written in terms of the equilibrium coordinates β_0, ϵ_0 and the parameters that characterize the system. Their final form is considerably involved. By way of example we present here only the form they assume for the case $\gamma = 0$ and $\psi = 0$. In this case the stability conditions are

$$A_1 > 0, \quad A_2 > 0, \quad A_3 > 0, \quad aA_0A_1A_3 > A_1(A_1A_2 - A_3A_4) + \frac{A_3^2}{12\alpha^2}, \tag{49}$$

where

$$A_0 = c(\alpha, X_0)f(\alpha, X_0) - d(\alpha, X_0)e(\alpha, X_0)$$

$$A_1 = f(\alpha, X_0) + \alpha\sigma c(\alpha, X_0) - \delta\left[X_0d(\alpha, X_0) + \alpha\frac{e(\alpha, X_0)}{X_0}\right]$$

$$A_2 = 2X_0\left\{c(\alpha, X_0)\left[-\frac{e(\alpha, X_0)}{X_0} + e'(\alpha, X_0)\right] - c'(\alpha, X_0)e(\alpha, X_0)\right\}$$

$$A_3 = \alpha\left\{c(\alpha, X_0)\left[-\frac{e(\alpha, X_0)}{X_0} + e'(\alpha, X_0)\right] - c'(\alpha, X_0)e(\alpha, X_0)\right\} + X_0\{f(\alpha, X_0)[c(\alpha, X_0) + X_0c'(\alpha, X_0)] - X_0d(\alpha, X_0)e'(\alpha, X_0)\}$$

$$A_4 = -2\frac{e(\alpha, X_0)}{X_0} + e'(\alpha, X_0) + X_0[c(\alpha, X_0) + X_0c'(\alpha, X_0)]\sigma + \delta\{c(\alpha, X_0) - X_0[c'(\alpha, X_0) + e'(\alpha, X_0)]\}$$

and $a = (\lambda^2\alpha)/(\kappa\beta_0^3 X_0^2)$. (50)

The expressions of (50) were evaluated by means of (39) and (40), and the stability of small motions was investigated numerically for a number of cases. In all these cases the conditions of (49) were found to be satisfied so that the equilibrium positions of (39) appear to be inherently stable in the presence of small disturbances.

Part 2: Numerical calculations and results

Numerical calculations for this study have two parts: (1) the calculation of equilibrium positions and the testing of each for stability; (2) the numerical integration of the two second-order ordinary differential equations of motion in order to investigate types of motion and stability in the large. The following section discusses the method used in (1), and the next discusses the methods used in (2) along with the errors involved in the calculations. In the concluding section typical results are presented and their implications discussed.

• *Equilibrium positions and stability in the small*

As shown in the concluding section of Part 1, equilibrium positions for the slider are found by solving (37) and (38), which are repeated below,

$$\kappa\alpha\frac{c(\alpha, X_0)}{\epsilon_0\beta_0} = \Pi + \alpha\gamma\beta_0 \tag{37}$$

and

$$\kappa\alpha^2\frac{e(\alpha, X_0)}{\epsilon_0^2} = \Phi - \psi\epsilon_0 \tag{38}$$

for β_0 and ϵ_0, where $X_0 = \epsilon_0/\beta_0$.

In most cases of physical interest, the terms $\gamma\beta_0$ and $\psi\epsilon_0$ are negligible. Consequently, the computations were performed only for the case where $\gamma = \psi = 0$. Under this assumption, the problem reduces to that of solving

$$\frac{e(\alpha, X_0)}{X_0^2} = \frac{\Phi}{\Pi\alpha}\frac{c(\alpha, X_0)}{X_0} \tag{51}$$

for X_0, and then finding β_0 and ϵ_0 from the relations

$$\beta_0^2 = \alpha\frac{\kappa}{\Pi}\frac{c(\alpha, X_0)}{X_0} \tag{52}$$

and

$$\epsilon_0 = X_0\beta_0. \tag{53}$$

Once an equilibrium position has been found it is a simple matter to calculate A_0, A_1, A_2, A_3, A_4 and a as defined in (50) and then check the inequalities in (49) to determine stability. (Note that the conditions in (49) also assume γ and ψ to be zero).

By writing (51) in the form

$$f(X_0) = \frac{\Phi}{\Pi\alpha}\frac{c(\alpha, X_0)}{X_0} - \frac{e(\alpha, X_0)}{X_0^2} = 0, \tag{54}$$

solutions may be obtained using the well-known Newton-Raphson iteration,

$$X_0^{(n+1)} = X_0^{(n)} - \frac{f(X_0^{(n)})}{f'(X_0^{(n)})}. \tag{55}$$

This method was found to be quite satisfactory; with an initial approximation of X_0 which differed from the true value by 20% or less the iteration usually converged to an accuracy of five significant figures in five or fewer iterations. However, there were some cases (usually where the slider was less stable) where an initial approximation of less than 20% from the solution was required to achieve convergence. As stated in Part 1, all equilibrium positions calculated were stable.

In some cases where the initial approximation was too far from the solution, a value of X_0 outside the interval [0, 1] was reached during the iteration. Such values are physically meaningless and in these cases the iterations were stopped. When rerun, these cases were always found to converge to values of X_0 in the interval [0, 1] when sufficiently close starting values were used.

• *Integration of the differential equations of motion*

To carry out the numerical integration of the equations of motion we first reduce the two second-order equations of (29) and (30) into the following system of four first-order equations.

$$\dot{\beta} = 12\alpha^2(\sigma y - \delta z) \tag{56}$$

$$\dot{\epsilon} = 12\alpha^2(\delta y - z) \tag{57}$$

$$\dot{y} = -\frac{\Pi}{\alpha} + \frac{\kappa}{\beta^2}\frac{c(\alpha, X)}{X} - \frac{\lambda}{\beta^3}12\alpha^2\left[\frac{\alpha c(\alpha, X)}{X^2}\cdot(\sigma y - \delta z) - \frac{d(\alpha, X)}{X}(\delta y - z)\right] \tag{58}$$

$$= -\frac{\Phi}{\alpha^2} + \frac{\kappa}{\beta^2}\frac{e(\alpha, X)}{X^2} - \frac{\lambda}{\beta^3}12\alpha^2\left[\alpha\frac{e(\alpha, X)}{X^3}\cdot(\sigma y - \delta z) - \frac{f(\alpha, X)}{X^2}(\delta y - z)\right]. \tag{59}$$

Two main considerations helped in choosing a numerical integration procedure for this system: First, because of the large amount of computation required for the

derivative evaluations, high order formulas permitting large time increments $\Delta\tau$ were desirable. In addition to reducing computing time, large time steps reduce the possibility of excessive round-off error. Second, since it is not possible to predict the behavior of the solutions, a built-in check on local truncation error is required so that the optimum step size can be determined by the program. This is the most practical way to minimize truncation and propagated error because no *a priori* choice for the step size can be made. Thus, $\Delta\tau$ is decreased when truncation error becomes too large and increased when the local error becomes very small, resulting in an efficient utilization of computer time.

Both Runge-Kutta and Predictor-Corrector methods were considered. R-K methods are desirable because they are self-starting and inherently stable. (The simple Euler P-C method is self-starting but is ruled out by the first consideration above.) However, a P-C method can be more easily and satisfactorily programmed to include automatic determination of the step size. (For one method of including error control with Runge-Kutta methods see pp. 238-239 of Reference 7.) The main objection to methods of the R-K type is that they require too many derivative evaluations. It was decided that a fourth-order method would be necessary to comply with the first consideration sited above. The standard fourth-order R-K formula requires four sets of derivative evaluations at each step. On the other hand, a fourth-order P-C method with the corrector applied only once requires two sets of derivative evaluations at each step. Experience has shown that applying the corrector only once is generally quite adequate and requires no significant decrease in step size. It was decided that a Predictor-Corrector method with the corrector applied only once, along with a Runge-Kutta method for starting, and restarting after a change in step size, would give the most satisfactory results.

It is desirable to choose a pair of P-C formulas which have error terms of opposite sign. For example, suppose that the calculated solution up through the value t_n of the independent variable is exactly correct. Then, if the error terms are of opposite sign, one knows that the true solution at t_{n+1} lies between the predicted and corrected values. Consequently, if the program selects a step size such that the predicted and corrected values differ by less than some δ, one can be sure that the corrected value differs from the true solution by less than δ. Of course, in an actual calculation the previous solution is not exactly correct and we are thus controlling only local truncation error with the hope of minimizing propagated error. The fourth-order Adams formulas have error terms of opposite sign and these were selected. All of the foregoing requirements are met by a SHARE program (RW INT). (This SAP-coded FORTRAN sub-routine was written in 1958 for Adams-Moulton, Runge-Kutta integration by R. Causey and W. L. Frank of Space Technology Laboratories.)

Let a general system of first-order equations be given in the form

$$\dot{y}_i = f_i(t, y_1, y_2, \cdots, y_N), \qquad \dot{y} = \frac{dy}{dt}, \tag{60}$$

with initial conditions of $y_i(t_0) = y_{i0}$, (61)

where $i = 1, 2, \cdots, N$.

If y_{in} equals y_i at $t = t_n$, f_{in} equals the derivative of y_i at $t = t_n$, and h is the step size of the independent variable t, the standard fourth-order Runge-Kutta formulas are

$$y_{i,n+1} = y_n + \tfrac{1}{6}(k_{i1} + 2k_{i2} + 2k_{i3} + k_{i4}) + O(h^5) \tag{62}$$

$$k_{i1} = h f_i(t_n, y_{1n}, y_{2n}, \cdots y_{Nn}) \tag{63}$$

$$k_{i2} = hf_i\left(t_n + \frac{h}{2}, y_{1n} + \tfrac{1}{2}k_{11}, y_{2n} + \tfrac{1}{2}k_{21}, \cdots, y_{Nn} + \tfrac{1}{2}k_{N1}\right) \tag{64}$$

$$k_{i3} = hf_i\left(t_n + \frac{h}{2}, y_{1n} + \tfrac{1}{2}k_{12}, y_{2n} + \tfrac{1}{2}k_{22}, \cdots, y_{Nn} + \tfrac{1}{2}k_{N2}\right) \tag{65}$$

$$k_{i4} = hf_i(t_n + h, y_{1n} + k_{13}, y_{2n} + k_{23}, \cdots, y_{Nn} + k_{N3}). \tag{66}$$

In the SHARE computer program these formulas are modified as proposed by Blum[8] to control the growth of round-off errors.

The Adams Predictor-Corrector formulas are

$$y^{(p)}_{i,n+1} = y_{in} + \frac{h}{24}(55f_{in} - 59f_{i,n-1} + 37f_{i,n-2} - 9f_{i,n-3}) + O(h^5) \tag{67}$$

$$y^{(c)}_{i,n+1} = y_{in} + \frac{h}{24}(9f_{i,n+1} + 19f_{in} - 5f_{i,n-1} + f_{i,n-2}) - O(h^5). \tag{68}$$

Double precision arithmetic is used in evaluating the Adams formulas since it reduces round-off error with a very small increase in computing time.

Examining (58) and (59) we see that to obtain an accurate solution, the functions $c(\alpha, X)$, $d(\alpha, X)$, $e(\alpha, X)$ and $f(\alpha, X)$ must be evaluated accurately before each set of derivative evaluations. We recall that physical considerations require $-\alpha/(1 - \alpha) \leq X \leq 1$. Examining the

four functions above it is clear that we need to look carefully at evaluations in the neighborhood of $X = 0$. From (35) and (36) one sees that $c(\alpha, X)/X^2$, $d(\alpha, X)/X$, $e(\alpha, X)/X^3$ and $f(\alpha, X)/X^2$ have finite limits as $X \rightarrow 0$. Hence,

$$\lim_{X\to 0} c(\alpha, X) = \lim_{X\to 0} d(\alpha, X) = \lim_{X\to 0} e(\alpha, X) = \lim_{X\to 0} f(\alpha, X) = 0. \quad (69)$$

It is clear, however, that these four functions, as they are written in Appendix 1, cannot be evaluated numerically for $X = 0$. Also, as X approaches zero some of the individual terms of the functions do not approach zero. These terms then cancel each other resulting in small values for the functions, and consequently in large losses in significant figures. The absolute error is even greater if $c(\alpha, X)$, $d(\alpha, X)$, $e(\alpha, X)$ and $f(\alpha, K)$ are calculated and stored and then the functions $c(\alpha, X)/X$, $c(\alpha, X)/X^2$, $d(\alpha, X)/X$, $e(\alpha, X)/X^2$, $e(\alpha, X)/X^3$ and $f(\alpha, X)/X^2$, which appear in (58) and (59), are calculated by dividing by the appropriate powers of X.

Two approaches can be taken to avoid these difficulties as $X \rightarrow 0$. The first approach and the most laborious requires expanding the logarithmic terms in power series and then writing the expressions for

$$c(\alpha, X),\quad c(\alpha, X)/X,\quad c(\alpha, X)/X^2,\quad d(\alpha, X),\quad d(\alpha, X)/X,$$
$$e(\alpha, X),\quad e(\alpha, X)/X^2,\quad e(\alpha, X)/X^3,\quad f(\alpha, X),\quad f(\alpha, X)/X^2, \quad (70)$$

so that they can be evaluated numerically for X near or equal to zero, without dividing by small numbers or causing the subtraction of very nearly equal terms. The second simply requires a determination of $\bar{\epsilon}$ such that for $|X| \geq \bar{\epsilon}$ the loss of accuracy is tolerable. Physically, this means not being able to study slider motions very close to or passing through the parallel position.

The second approach was taken because sufficient information could be obtained without considering motions close to the parallel position. The functions $c(\alpha, X)$, $d(\alpha, X)$, $e(\alpha, X)$ and $f(\alpha, X)$ were programmed very much as they appear in Appendix 1. The four functions are calculated and stored and then the necessary divisions by powers of X are made as needed. Some tabulations were made of the ten functions in (70). The results showed that X can get close to zero before loss of accuracy becomes excessive. After examining $c(\alpha, X)$, $d(\alpha, X)$, $e(\alpha, X)$ and $f(\alpha, X)$ and the tabulations of (70), it was decided that for $|X| \geq 0.1$, the losses of accuracy in calculating the functions of (70) are two significant figures or less. (In the computer used, floating point arithmetic gives eight significant digits).

It should be noted that in the Newton-Raphson iteration discussed in the previous section on equilibrium conditions the same difficulties with loss of accuracy are present because (54) involves $c(\alpha, X_0)$ and $e(\alpha, X_0)$. With only $c(\alpha, X_0)$ and $e(\alpha, X_0)$ involved, however, the loss of accuracy is two significant figures or less for $X_0 \geq 0.05$. In the equilibrium positions calculated, X_0 was always much greater than 0.05.

The integration program was designed to stop when any of the following three conditions occur: $|X| < \bar{\epsilon}$; $X \geq 1$; or $X \leq -\alpha/(1-\alpha)$. None of these conditions were encountered in the trajectories computed.

Even if the functions $c(\alpha, X)$, $d(\alpha, X)$, $e(\alpha, X)$ and $f(\alpha, X)$ were evaluated with no error, there would still be error as a result of the integration procedure itself. As stated above, the integration program has a built-in error control which operates as follows: At each time step, if δ equals the maximum of the absolute values of the differences between the predicted and corrected values for β, ϵ, y, and z, then the step size is suitably chosen so that $\underline{e} \leq \delta \leq \bar{e}$ where $\underline{e}$ and $\bar{e}$ are input parameters. For all the trajectories computed $\bar{e} = 10^{-6}$ and $\underline{e} = 10^{-8}$. The accuracy yielded by these bounds was investigated by computing a trajectory several times using a smaller and smaller fixed step size and comparing the results with those obtained using the variable step size.

The trajectory studied is shown as Fig. 2, page 313. The greatest motion occurs near $\tau = 0$ and then diminishes as τ increases. Therefore, near $\tau = 0$ truncation error is dominant, whereas as τ increases, it is propagated error due to round-off that becomes more significant. Table 1 shows tabulations of ϵ and β at $\tau = 0.125$, 0.25, and 1.0 for several fixed step sizes and for the variable step mode, in which $\Delta\tau$ ranges from 0.015625 to 0.0625. One will notice that for the largest step size, 0.125, there are no entries for $\tau = 1.0$. This is because 0.125 is too large for the motion near $\tau = 0$ and, consequently, the truncation error became so great that X exceeded its upper bound causing the program to stop at $\tau = 0.5$.

Examining Table 1 we see that all the variable step entries for ϵ and β agree to at least five significant figures with the entries for the smallest three step sizes. Thus, it appears that $\bar{e} = 10^{-6}$ assures at least five figures of accuracy for this trajectory. Trajectories with larger motions than those in Fig. 2 generally used somewhat fewer time steps (meaning that truncation error becomes more important), while the trajectories showing overdamping required more time steps (meaning that propagated error becomes more significant). However, the two most extreme cases required, on the one hand, more than two-thirds as many and, on the other, fewer than three times as many time steps as did the case illustrated in Fig. 2. Consequently, it appears that $\bar{e} = 10^{-6}$ ensures sufficient accuracy for all the trajectories since no more than three significant figures are required.

Table 1 **Values of ϵ and β for fixed step sizes and the variable step mode.**

$\Delta\tau$	$\epsilon \times 10^3$	$\beta \times 10^3$
At τ = 0.125:		
0.125	1.7658884	4.2506446
0.0625	1.7414479	4.3083826
0.03125	1.7399853	4.3113894
0.015625	1.7400383	4.3112939
0.0078125	1.7400369	4.3112913
0.00390625	1.7400362	4.3112913
Variable	1.7400383	4.3112939
At τ = 0.25:		
0.125	1.8539759	4.0761222
0.0625	1.8274397	4.1167538
0.03125	1.8236381	4.1187019
0.015625	1.8237691	4.1182705
0.0078125	1.8237747	4.1182519
0.00390625	1.8237742	4.1182510
Variable	1.8237691	4.1182705
At τ = 1.0:		
0.125	——	——
0.0625	1.5848905	3.8453113
0.03125	1.5844493	3.8449128
0.015625	1.5844424	3.8449055
0.0078125	1.5844413	3.8449051
0.00390625	1.5844411	3.8449054
Variable	1.5844628	3.8449122

• *Results and comments*

The computer programs we have mentioned can be used for the determination of equilibrium positions and motion trajectories of the slider for various combinations of the parameters α, δ, κ, λ, Π, Φ and arbitrary initial conditions β_i, ϵ_i, $\dot{\beta}_i$, $\dot{\epsilon}_i$. A number of runs has been completed and a set of typical results is presented in Figs. 2-10. The parameter values and initial conditions used in the corresponding calculations are set forth in Table 2. The initial conditions chosen were the same for all cases, i.e.,

$$\beta_i = 1.2\beta_0, \qquad \epsilon_i = \epsilon_0, \qquad \dot{\beta}_i = 0 = \dot{\epsilon}_i. \tag{71}$$

Note that the results apply to a bearing without rotary stiffness in the suspension system so that the parameter Φ has the value zero. The parameter-values used in the example of Fig. 2 describe a bearing with physical parameters $B = 1.0$ in., $b = 0.4$ in., $p_a = 14.7$ psi, $U = 2000$ ips, $\mu = 2.62 \times 10^{-9}$ lb sec/in^2, $m = 3.0 \times 10^{-5}$ lb sec^2/in^2, $K = 1.0$ lb/in and $Q = 0$. From the definition $\tau = \omega t = t\sqrt{p_a/m}$ the time-scale in Fig. 2 is thus given by the relation $\tau = 700\ t$, where t is expressed in seconds.

The system of Fig. 2 is arbitrarily identified as the typical system and succeeding examples are obtained by making one single change in the values of the physical parameters for the typical case. The same time scale, $\tau = 700\ t$, thus applies to all examples except that represented by Fig. 10, which is obtained by increasing the mass of the typical slider by a factor of ten. It follows that the time-scale in Fig. 10 is defined by the relation $\tau = 221.36\ t$ where t is expressed in seconds.

Figures 2-10 present the equilibrium positions (β_0, ϵ_0) and the motion trajectories $(\beta(\tau), \epsilon(\tau))$ for the cases considered. The trajectories show an instantaneous coupling

Table 2 **Parameters and initial conditions for calculation of motion trajectories in Figs. 2-10. (For all Figures $\Phi = 0$.)**

Figure Number	*Parameter values and initial conditions:* α	δ	$\kappa \times 10^6$	$\lambda \times 10^6$	Π	σ	$\epsilon_0 \times 10^3$	$\epsilon_i \times 10^3$	$\beta_0 \times 10^3$	$\beta_i \times 10^3$
2	0.4	−0.25	2.1388	1.4971	0.068027	0.58333	1.5864	1.5864	3.8241	4.5889
3	0.2	−1.5	2.1388	1.4971	0.068027	4.3333	7.5901	7.5901	8.5140	10.217
4	0.4	0.25	2.1388	1.4971	0.068027	0.58333	1.5864	1.5864	3.8241	4.5889
5	0.4	−0.25	2.1388	1.4971	0.034014	0.58333	2.2434	2.2434	5.4080	6.4896
6	0.4	−0.25	2.1388	1.4971	0.0068027	0.58333	5.0165	5.0165	12.093	14.511
7	0.4	−0.25	2.1388	1.4971	0.13605	0.58333	1.1217	1.1217	2.7040	3.2449
8	0.4	−0.25	1.0694	1.4971	0.068027	0.58333	1.1217	1.1217	2.7040	3.2449
9	0.4	−0.25	3.2082	1.4971	0.068027	0.58333	1.9429	1.9429	4.6835	5.6202
10	0.4	−0.25	2.1388	0.47344	0.068027	0.58333	1.5864	1.5864	3.8241	4.5889

of the translational and rotational motions in all cases. Figure 2 shows that the transient response of the typical system is aperiodical and that a disturbance of the type described by (71) dies out within about 2 milliseconds. As shown in Fig. 3, a considerable change in behavior occurs when the pivot point is moved towards the trailing edge. The system damping is greatly reduced, the response becomes oscillatory, and superharmonics become apparent. The fundamental period of oscillation in this case is about 3.4 milliseconds. Note that the equilibrium coordinates β_0 and ϵ_0 are much greater than those for the typical case and that the ratio $\epsilon_0/\beta_0 = X_0$ has also increased. This explains to some extent the decrease of system damping and stiffness involved in moving the pivot point towards the trailing edge. From the equations of motion, (29) and (30) and from the data of Appendix 1, it follows that the terms representing damping and stiffness of the lubricating film are inversely proportional, respectively, to factors of the form $X_0^m\beta_0^3$ and of the form $X_0^n\beta_0^2$, with $m > 0$ and $n > 0$; hence, with both X_0 and β_0 increasing, both the damping and the stiffness of the film must decrease rapidly. If X_0 were to remain constant, the effective damping of the lubricating film would decrease or increase, relative to the effective stiffness, according to whether the thickness would increase or decrease.

Figure 2 **The typical case. Parameters are as given on page 312.**

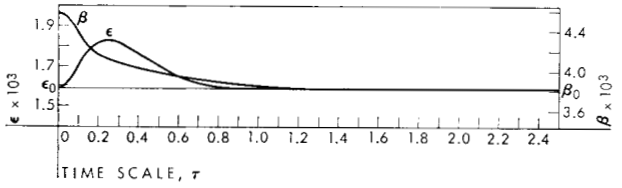

Figure 3 **Case with pivot moved 0.2 inch toward trailing edge.**

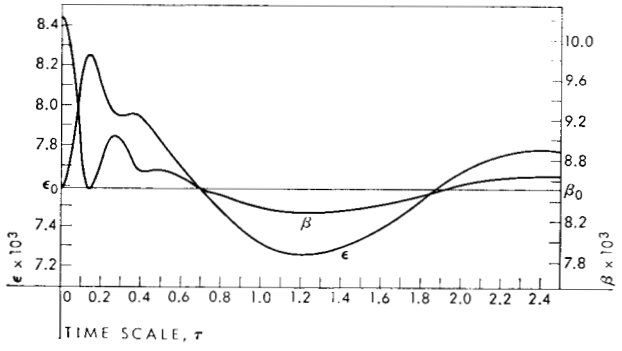

Figure 4 **Case with center of gravity moved toward trailing edge.**

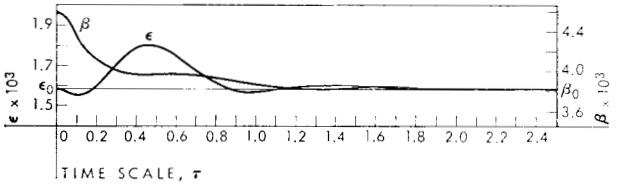

Figure 5 **Case with load decreased by 50 per cent.**

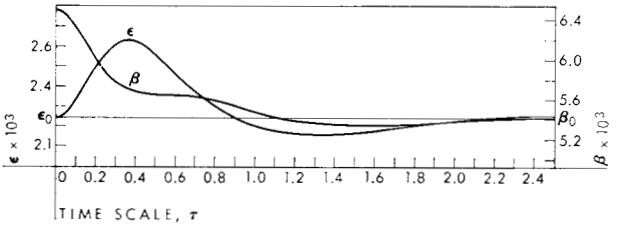

In the example of Fig. 3 the pivot point is moved a distance of 0.2 inch toward the trailing edge. Figure 4 shows that when the center of gravity is moved an equal distance toward the trailing edge, while keeping the pivot point in the same position as for the typical case, the effect is then much smaller. The response is similar to that of the typical system, even though the damping is somewhat reduced and some oscillatory motion becomes apparent. The reduction in system damping and stiffness here involved can now not be ascribed to a change in the values of X_0 and β_0, since it is clear from Figs. 2 and 4 that the equilibrium positions β_0 and ϵ_0 are not altered. This also follows for these positions from (39) and (40) and from the fact that they do not contain the parameter δ; this parameter is the only one affected, while in the previous example both α and δ were involved. Since the other parameters occurring in the damping and stiffness terms of the equations of motion are similarly unaltered, the change in film damping and stiffness for varying values of δ can be explained only by considering the behavior and relative magnitudes of the coefficient functions $c(\alpha, X)$, $d(\alpha, X)$, $e(\alpha, X)$ and $f(\alpha, X)$ listed in Appendix 1. These functions are, however, too involved for detailed consideration here.

Figures 5, 6, and 7 show the motion trajectories of the slider for, respectively, a 50% decrease, a 90% decrease and a 100% increase in load compared with the typical system. In Fig. 5 the response is still aperiodic although the motion appears to be on the verge of oscillation. This implies, of course, that reducing the load has reduced both the film damping and film stiffness as one would expect. Figure 6 makes this trend abundantly clear, while Fig. 7 illustrates the fact that the opposite effect occurs if the load is increased. It will be observed that

the values of β_0 and ϵ_0 are different in all three cases (greater than those for the typical case if the load is reduced and vice versa) but that the ratio $\epsilon_0/\beta_0 = X_0$ remains constant. That this should be the case follows directly from (39) for the equilibrium positions; for the case under consideration here, where $\Phi = 0$, this equation becomes simply $e(\alpha, X_0) = 0$. If α remains unchanged, so does the ratio ϵ_0/β_0. From (40), the second equation for the equilibrium positions, it is clear that, for a fixed value of κ, β_0^2 is inversely proportional to Π. Moreover, with λ also kept constant, it follows from (29) and (30), the two equations of motion, that the film damping in this case is proportional to $\Pi^{3/2}$ and the film thickness is proportional to Π. Thus, for a 50% reduction in load, as shown in Fig. 5, the film damping is reduced by a multiplication factor of $(1/2)^{3/2} = 0.354$, and the stiffness by a factor of 0.5. For a 90% reduction in load (Fig. 6) these factors are 0.0316 and 0.1 respectively, while for a 100% increase in load (Fig. 7) damping and stiffness should be increased by factors of 2.83 and 2.0, respectively. The Figures bear out these observations, at least qualitatively. Note that the fundamental period in the example of Fig. 6 is about 12 milliseconds.

Figures 8 and 9 show the effect of variations in speed of the driving surface. These figures apply respectively to a 50% decrease and a 50% increase in the magnitude of the driving surface speed U, that is, of the parameter κ. Note that X_0 also remains constant in this case and, from Eq. (40), that β_0^2 is proportional to κ. It follows from the equations of motion, (29) and (30), that the stiffness of the lubricating film is not affected but that the damping is varied by a factor proportional to $\kappa^{-3/2}$. Compared with the typical case of Fig. 2 the system damping in Fig. 8 is thus increased by the factor $2^{3/2}$ (i.e., 2.83), while in Fig. 9 the damping is decreased by the factor $(2/3)^{3/2}$ (i.e., 0.545). These observations are borne out by the Figures. Note also the similarity between the trajectories of Figs. 5 and 9, and that between the trajectories of Figs. 7 and 8. The latter two Figures represent, respectively, the effect of doubling the load and halving the driving speed; hence the value of the parameter Π is doubled and the value of the parameter κ is halved. It follows from Eq. (40) that the effect of these changes on β_0 is identical, so that the film damping is increased an equal amount in both cases. In the case of Figs. 5 and 9, the former shows the effect of halving the value of Π, hence doubling β_0^2, while the latter shows the effect of multiplying κ, hence β_0^2, by a factor of 1.5. Compared with the typical case of Fig. 2 the film damping is thus reduced by a factor of about one-third in the first case, and about one-half in the second. These observations agree quite well with the trajectories shown in Figs. 5 and 9.

The effect of changing the mass of the slider is illustrated in Fig. 10. The only parameter affected in this case

Figure 6 **Case with load decreased by 90 per cent.**

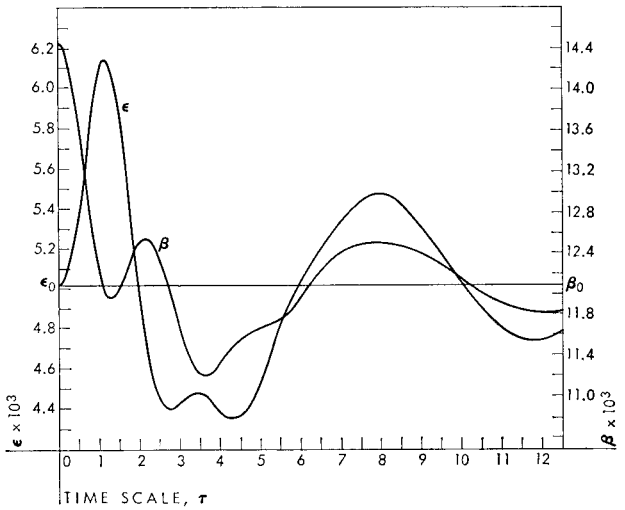

Figure 7 **Case with load increased by 100 per cent.**

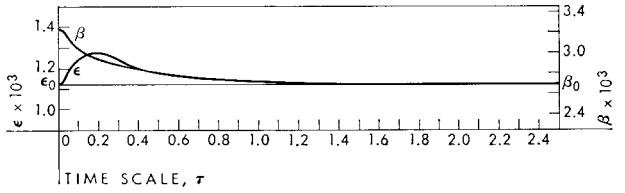

Figure 8 **Case with driving surface velocity decreased by 50 per cent.**

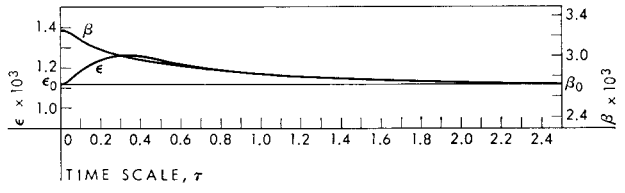

Figure 9 **Case with driving surface velocity increased by 50 per cent.**

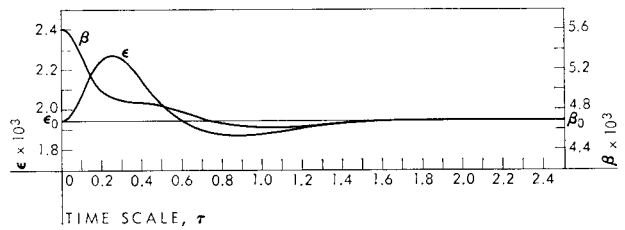

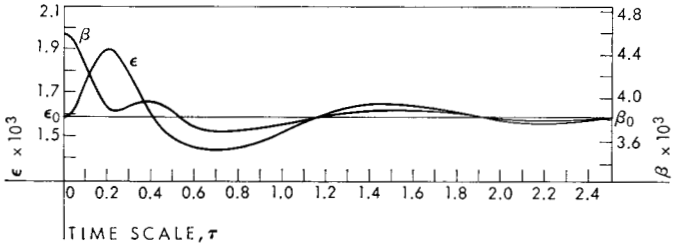

Figure 10 **Case with mass increased by a factor of 10.**

is λ, which is inversely proportional to $\sqrt{m}$. Equations (39) and (40) show that the equilibrium positions β_0 and ϵ_0 are not affected, hence X_0 is unaffected, and the change in system behavior is thus solely due to the change in λ. Consequently, the stiffness of the film remains the same and, for an increase in mass by a factor of 10, the damping is reduced to about one-third its original value (see Fig. 2). It follows from Fig. 10 that the fundamental period in this case is about 7 milliseconds; it may be noted that the relation $\tau = 221.36t$ applies in this case.

Acknowledgments

The authors are indebted to W. A. Michael for pointing out an error in the original manuscript, and gratefully acknowledge valuable suggestions, support, and comments received from him and from W. A. Gross.

Appendix 1 Definitions of the functions $c(\alpha, X)$, $d(\alpha, X)$, $e(\alpha, X)$, and $f(\alpha, X)$.

$$c(\alpha, X) = \frac{-2}{\alpha[2\alpha + (1 - 2\alpha)X]} + \frac{1}{\alpha X} \ln\left[1 + \frac{X}{\alpha(1 - X)}\right].$$

$$e(\alpha, X) = -\frac{6\alpha + (1 - 2\alpha)X}{2\alpha^2[2\alpha + (1 - 2\alpha)X]} + \frac{3\alpha + 2(1 - 2\alpha)X - (1 - \alpha)X^2}{\alpha X[2\alpha + (1 - 2\alpha)X]} \cdot \ln\left[1 + \frac{X}{\alpha(1 - X)}\right]$$

Defining

$$Q_0(\alpha, X) = \frac{2}{\alpha} \cdot \frac{2X - \alpha\left[(1 - X)^2 \ln(1 - X) - \left(1 + \frac{1 - \alpha}{\alpha} X\right)^2 \ln\left(1 + \frac{1 - \alpha}{\alpha} X\right)\right]}{(1 - X)^2 - \left(1 + \frac{1 - \alpha}{\alpha} X\right)^2}$$

$$Q_1(\alpha, X) = \left(1 + \frac{1 - \alpha}{\alpha} X\right)^2 [(-3 + 4X) - 2(1 - X)^2 \ln(1 - X)]$$
$$+ \frac{(1 - X)^2\left[\left(3 + 4\frac{1 - \alpha}{\alpha} X\right) + 2\left(1 + \frac{1 - \alpha}{\alpha} X\right)^2 \ln\left(1 + \frac{1 - \alpha}{\alpha} X\right)\right]}{(1 - X)^2 - \left(1 + \frac{1 - \alpha}{\alpha} X\right)^2}.$$

Then

$$d(\alpha, X) = \frac{1}{4\alpha X^3}\left\{X\left[Q_0(\alpha, X) - 2 - \frac{Q_1(\alpha, X) + 1}{(1 - X)\left(1 + \frac{1 - \alpha}{\alpha} X\right)}\right]\right.$$
$$\left. - 2\alpha\left[(3 - X)\ln(1 - X) - \left(3 + \frac{1 - \alpha}{\alpha} X\right)\ln\left(1 + \frac{1 - \alpha}{\alpha} X\right)\right]\right\}$$

And $$f(\alpha, X) = \frac{1}{4\alpha X^3}\left\{-6X - \frac{1-2\alpha}{2\alpha}\cdot X^2\cdot Q_0(\alpha, X) - \frac{[Q_1(\alpha, X)+1]X}{(1-X)\left(1+\frac{1-\alpha}{\alpha}\cdot X\right)}\right.$$

$$-\frac{\alpha}{2}\left[(1-X)^2 - \left(1+\frac{1-\alpha}{\alpha}\cdot X\right)^2\right] + \alpha X^2\left[\ln(1-X) - \left(\frac{1-\alpha}{\alpha}\right)^2 \ln\left(1+\frac{1-\alpha}{\alpha}\cdot X\right)\right]$$

$$\left.-\alpha[Q_1(\alpha, X)+6]\left[\ln(1-X) - \ln\left(1+\frac{1-\alpha}{\alpha}X\right)\right]\right\}$$

Appendix 2 Definitions of the coefficient functions in Eqs. (43) and (44).*

$$A = \frac{\alpha}{\beta_0^3}\cdot\frac{c(\alpha, X_0)}{X_0^2}$$

$$B = \frac{1}{\beta_0^3}\cdot\frac{d(\alpha, X_0)}{X_0}$$

$$C = \frac{1}{\beta_0^3}\left[\frac{c(\alpha, X_0)}{X_0} + c'(\alpha, X_0)\right]$$

$$D = \frac{1}{\beta_0^3}\cdot\frac{1}{X_0}\left[-\frac{c(\alpha, X_0)}{X_0} + c'(\alpha, X_0)\right]$$

$$P = \frac{\alpha}{\beta_0^3}\cdot\frac{e(\alpha, X_0)}{X_0^3}$$

$$Q = \frac{1}{\beta_0^3}\cdot\frac{f(\alpha, X_0)}{X_0^2}$$

$$R = \frac{1}{\beta_0^3}\cdot\frac{1}{X_0}\cdot e'(\alpha, X_0)$$

$$S = \frac{1}{\beta_0^3}\cdot\frac{1}{X_0^2}\left[-2\frac{e(\alpha, X_0)}{X_0} + e'(\alpha, X_0)\right]$$

* In all cases primes indicate differentiation with respect to X_0.

References

1. Capriz, G., "On Some Dynamical Problems Arising in the Theory of Lubrication," *Rivista di Mathematica della Universita di Parma* **1**, No. 2, 1960, (1-20).
2. Kestens, J., "Stabilité de la Position de l'Arbre dans un Palier à Graissage Hydrodynamique," *Wear* **2**, 329-357, 1960.
3. "A Gas Film Lubrication Study," *IBM Journal* **3**, 237-274 (1959).
4. Gross, W. A., *Gas Film Lubrication*, John Wiley and Sons, New York, 1962.
5. Langlois, W. E., "Isothermal Squeeze Films," *Quarterly of Applied Mathematics* **20**, 2, (1962).
6. Minorsky, N., *Introduction to Non-Linear Mechanics*, J. W. Edwards, Ann Arbor, 1947, pp. 153-158.
7. Hildebrand, F. B., *Introduction to Numerical Analysis*, McGraw-Hill, New York, 1956, pp. 188-257.
8. Blum, E. K., "A Modification of the Runge-Kutta Fourth-Order Method," *Appendix H, Proc. Math. Committee of Univac Scientific Exchange Meeting*, November 21-22, 1957.

Received December 1, 1962